Radial Collateral Ligament of the Elbow

Sonographic Characterization With Cadaveric Dissection Correlation and Magnetic Resonance Arthrography

Jon A. Jacobson, MD, Mary M. Chiavaras, MD, PhD, Jason Michael Lawton, Brian Downie, PA-C, Corrie M. Yablon, MD, Jeffrey Lawton, MD

Objectives—An abnormality of the radial collateral ligament (RCL) in the setting of lateral epicondylitis can indicate a poor clinical outcome; therefore, accurate assessment is important. The purpose of this study was to characterize the proximal RCL attachment, or footprint, as seen on sonography using cadaveric dissection correlation and magnetic resonance arthrography.

Methods—For the first part of this study, 4 cadaveric elbow specimens were imaged with sonography before and after dissection to characterize the RCL. After Institutional Review Board approval with consent waived, 26 consecutive magnetic resonance (MR) arthrograms of the elbow were identified. The sonograms and MR arthrograms were retrospectively reviewed to measure the length of the RCL footprint and its percentage of the combined RCL and common extensor tendon (CET) humeral footprints.

Results—The mean RCL footprint length and percentage of the combined RCL and CET footprints were 8.4 mm (range, 7.4–10.0 mm) and 54% as measured from the elbow specimen sonograms and 9.1 mm (range, 6.4–12.5 mm) and 54% as measured from the MR arthrograms. The mean RCL footprint length combining data from specimens and MR arthrograms was 8.9 mm (range, 6.4–12.5 mm), covering 54% of the combined RCL and CET footprints.

Conclusions—The RCL can be differentiated from the CET on sonography with knowledge of the RCL humeral footprint extent, which measured 8.9 mm in length and comprised 54% of the combined RCL and CET footprints.

Key Words—common extensor tendon; elbow; magnetic resonance arthrography; magnetic resonance imaging; musculoskeletal ultrasound; radial collateral ligament; sonography

Lateral epicondylitis, or tennis elbow, is the most common cause of lateral elbow pain and can be a major cause of symptoms and debilitation.[1] The term "lateral epicondylitis" is a misnomer, in that the abnormality causing tennis elbow is degeneration and a possible tear of the common extensor tendon (CET) at or near its humeral origin.[2] Histologic studies have shown that there is no significant inflammation associated with chronic tennis elbow; therefore, the term "tendinitis" is not appropriate.[3] Moreover, hyperemia on color and power Doppler imaging has been shown to represent neovascularity and not inflammation.[3]

Sonography and magnetic resonance imaging (MRI) may be used to confirm clinically suspected tennis elbow and to exclude other causes of lateral elbow pain.[1,2] Such imaging can reveal the extent of the tendon abnormality and also show a coexisting abnormality of the radial collateral ligament (RCL), which lies immediately

Received June 26, 2013, from the Departments of Radiology (J.A.J., B.D., C.M.Y.) and Orthopedic Surgery (J.M.L., J.L.), University of Michigan, Ann Arbor, Michigan USA; and Department of Diagnostic Imaging, McMaster University, Hamilton General Hospital, Hamilton, Ontario, Canada. Revision requested July 17, 2013. Revised manuscript accepted for publication September 30, 2013.

We thank Quinn Burrell for the Figure 1 illustration.

Address correspondence to Jon A. Jacobson, MD, Division of Musculoskeletal Radiology, Department of Radiology, University of Michigan, 1500 E Medical Center Dr, TC2910L, Ann Arbor, MI 48109-0326 USA.

E-mail: jjacobsn@umich.edu

Abbreviations

CET, common extensor tendon; MR, magnetic resonance; MRI, magnetic resonance imaging; RCL, radial collateral ligament; TE, echo time; TR, repetition time; TSE, turbo spin echo

doi:10.7863/ultra.33.6.1041

deep and adjacent to the CET (Figure 1).[2,4] In the setting of tennis elbow, an abnormality of the lateral ulnar collateral ligament of the RCL complex has been described in up to 63% of cases.[5] The presence of an RCL tear in the setting of lateral epicondylitis is also associated with a poor clinical outcome after nonsurgical management.[4,6] In addition, understanding the normal appearance of the RCL is required to diagnose RCL abnormalities; therefore, accurate characterization of the anatomy and pathologic characteristics of the lateral elbow is important.

In our clinical practice, sonography is used to evaluate the lateral elbow for CET abnormalities. We have noted difficulty in defining the RCL and CET as separate structures when characterizing disorders associated with tennis elbow. The purpose of this study was to characterize the RCL footprint and its relationship with the CET footprint on the lateral epicondyle of the humerus using both sonography with cadaveric dissection and magnetic resonance arthrography.

Figure 1. Lateral elbow showing the RCL (blue), which extends from the humerus (H) to the annular ligament (A). The overlying CET and muscle (E) orientation is slightly oblique to the RCL. Note the lateral ulnar collateral ligament (curved arrow) and its attachment to the ulna (U). R indicates radius.

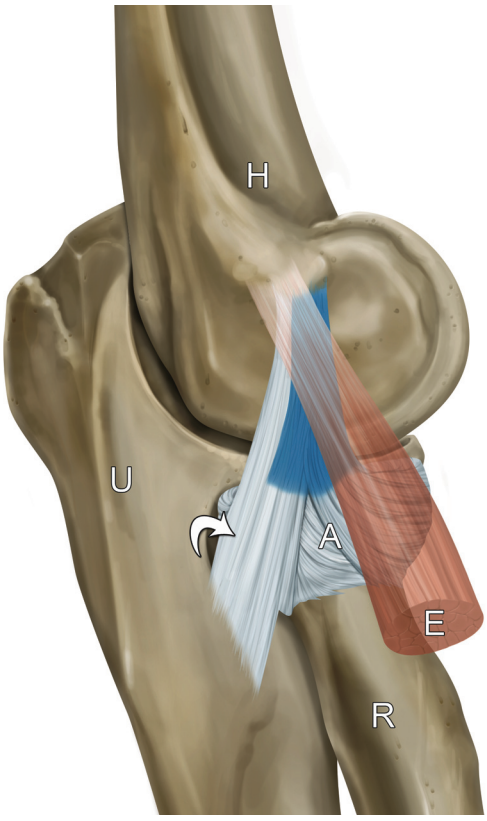

Materials and Methods

This study was divided into the following 2 parts: (1) dissection of 4 cadaver elbows and subsequent sonography both before and after dissection; and (2) retrospective review of MR arthrograms of the elbow. The purpose was to identify the RCL and to characterize its humeral attachment, or footprint.

Cadaveric Dissection and Sonography

Approval for this portion of the study was obtained by the Anatomical Donations Department at our institution. Four fresh nonembalmed elbow specimens were obtained, and each lateral elbow was imaged in extension with sonography by a musculoskeletal fellowship-trained radiologist (18 years of experience in musculoskeletal sonography) using a 12-MHz linear transducer (iU22; Philips Healthcare, Bothell, WA). Specifically, long- and short-axis images of the RCL and CET were obtained and recorded, including cine clips. On sonography, a normal tendon appears as a hyperechoic fibrillar structure, and a normal ligament appears as a compact hyperechoic fibrillar structure.[7] Both structures may appear artifactually hypoechoic if not imaged perpendicular to the ultrasound beam due to anisotropy.

Subsequently, each elbow was dissected by a fellowship-trained orthopedic upper extremity surgeon (14 years of experience in elbow surgery). For each elbow, the skin, subcutaneous tissues, and fascia were removed to expose the CET over the lateral elbow. The CET was then identified, isolated, and then released from its humeral origin and retracted, revealing the underlying RCL. The specimen was then placed in a water bath and again imaged with sonography by the same radiologist using the same equipment. Long- and short-axis images of the RCL, including cine clips, were again obtained.

The sonograms from the cadavers were then reviewed, both before and after CET removal, in consensus by 2 fellowship-trained radiologists (with 18 and 2 years of experience). The length of the isolated RCL humeral footprint (ie, after CET removal) was measured in the long axis relative to the ligament fibers on a computer station using digital calipers, and the data were recorded. The combined RCL and CET footprint length was also measured and recorded.

Magnetic Resonance Arthrography Review

After Institutional Review Board approval, consecutive elbow MR arthrographic studies completed in 2010 and 2011 were identified. The arthrographic studies were completed as part of routine patient care on a 3-T MRI system (Achieva; Philips Healthcare, Andover, MA) after the

intra-articular administration of a diluted gadolinium contrast agent (gadopentetate dimeglumine; Magnevist; Bayer Schering, Berlin, Germany) using fluoroscopy from a lateral approach via the radiocapitellar joint or using fluoroscopy or sonography from a posterior approach through the triceps brachii. The MRI sequences included coronal T1-weighted turbo spin echo (TSE) images (repetition time [TR]/echo time [TE], 500–800/10 milliseconds; echo train length, 4; flip angle, 90°; slice thickness, 2.5 mm; matrix, 528) without and with fat saturation, coronal T2-weighted fat-saturated TSE images (TR/TE, 2000–6000/40 milliseconds; echo train length factor, 10; flip angle, 90°; slice thickness, 2.5 mm; matrix, 528), axial T1-weighted TSE images (TR/TE, 500–800/10 milliseconds; echo train length factor, 4; flip angle, 90°; slice thickness, 2.5 mm; matrix, 528), axial T2-weighted fat-saturated TSE images (TR/TE, 2000–6000/40 milliseconds; echo train length factor, 10; flip angle, 90°; slice thickness, 2.5 mm; matrix, 528), and sagittal T1-weighted fat-saturated TSE images (TR/TE, 500–800/30 milliseconds; echo train length factor, 4; flip angle, 90°; slice thickness, 2.5 mm; matrix, 512).

The MR arthrograms were reviewed by 2 fellowship-trained radiologists in consensus (with 18 and 2 years of experience). Exclusion criteria included an abnormal increased signal in the RCL. The RCL footprint length was measured in the long axis relative to the ligament fibers on the coronal T1-weighted sequence at a computer station using digital calipers, and the data were recorded. The combined RCL and CET footprint length was also measured and recorded. The footprints of the RCL and CET were identified by directly visualizing the ligament and tendon fiber attachments to the humerus, respectively.

Statistical Analysis

Radial collateral ligament footprint lengths (measured in the long axis to the RCL) were evaluated for normality, and then the mean, standard error of the mean (SEM), and 95% confidence intervals for the two groups (sonography and MR arthrography) were calculated. The RCL lengths measured from these groups were then compared by the Student *t* test (SAS version 9.2; SAS Institute Inc, Cary, NC).

Results

Cadaveric Dissection and Sonography

With regard to the 4 cadaveric elbow specimens, the mean age was 72 years (range, 62–82 years). Causes of death were not known. Sonographic evaluation of each lateral elbow before dissection did not show any abnormality of the CET or RCL.

Retrospective review of the sonograms from the 4 cadaveric specimens after removal of the CET revealed a mean RCL footprint length of 8.4 mm (range, 7.4–10.0 mm; SEM, 0.56789 mm; 95% confidence interval, 7.01–9.69 mm; Table 1 and Figures 2 and 3). The RCL footprint length in the long axis comprised, on average, 54% of the combined RCL and CET long-axis footprints on the proximal humerus (mean length, 15.4 mm; range, 14.8–15.4 mm; Table 1).

Magnetic Resonance Arthrography Review

On MR arthrograms, the normal RCL appears as a homogeneous low-signal structure that extends from the humerus to the annular ligament lying just deep to the CET (Figures 4 and 5). The normal CET appears as a homogeneous low-signal structure lying immediately superficial to the RCL with a more proximal attachment to the lateral epicondyle of the humerus (Figures 4 and 5). An initial search of our radiology information system identified 30

Table 1. Humeral Footprint Lengths by Imaging Method

Imaging Method	RCL Footprint Length, mm	Combined RCL + CET Footprint Length, mm	RCL as % of Total Footprint
Sonography	10.0	16.2	62
Sonography	7.4	15.3	48
Sonography	8.0	14.8	54
Sonography	8.0	15.4	52
MR arthrography	7.2	17.3	42
MR arthrography	7.5	17.6	43
MR arthrography	7.1	13.7	52
MR arthrography	8.6	15.2	57
MR arthrography	8.9	15.5	57
MR arthrography	10.4	19.0	55
MR arthrography	8.1	15.2	53
MR arthrography	8.0	16.0	50
MR arthrography	7.8	16.0	49
MR arthrography	8.1	16.5	49
MR arthrography	10.6	20.4	52
MR arthrography	8.9	17.2	52
MR arthrography	12.5	21.0	60
MR arthrography	8.5	20.3	42
MR arthrography	7.9	11.7	68
MR arthrography	10.5	17.7	59
MR arthrography	9.4	17.0	55
MR arthrography	6.4	11.3	57
MR arthrography	8.9	17.4	51
MR arthrography	8.9	18.8	47
MR arthrography	11.4	19.1	60
MR arthrography	11.5	17.9	64
MR arthrography	8.1	16.0	51
MR arthrography	8.9	13.6	65
MR arthrography	10.2	16.7	61
MR arthrography	9.7	18.9	51

patients. After exclusion of patients with abnormal signal in the RCL, the final study group consisted of 26 patients (21 male and 5 female) with a mean age of 19 years (range, 13–36 years). The right elbow was imaged in 81% (21 of 26) and the left in 19% (5 of 26). The joint injection was completed by a lateral approach with fluoroscopy (radiocapitellar) in 58% (15 of 26) and a posterior approach (through the triceps brachii) in 42% (11 of 26) with fluoroscopy in 9 and sonography in 2. Patient histories included evaluations for ulnar collateral ligament tears in 19, evaluations for osteochondral abnormalities in 5, and nonspecific elbow pain in 2.

Retrospective review of the coronal T1-weighted MR arthrograms showed the CET superficial to the RCL (Figures 4 and 5). The mean RCL footprint length in the long axis measured 9.1 mm (range, 6.4–12.5 mm; SEM, 0.2923 mm; 95% confidence interval, 8.5–9.49 mm; Table 1 and Figure 4) and comprised, on average, 54% of the combined RCL and CET footprints (mean length, 16.8 mm; range, 11.3–21.0 mm; Table 1).

Taken collectively, the cadaveric specimens and patients who underwent MR arthrography had a mean RCL footprint length of 8.9 mm (range, 6.4–12.5 mm), covering an average of 54% (range, 11.3–21.0 mm) of the combined RCL and CET footprints. The Student *t* test showed no statistical difference between the RCL lengths measured from the arthrograms and sonograms ($t = 1.02$; $P = .3577$).

Discussion

Accurate imaging characterization of CET abnormalities in the setting of tennis elbow is important, as involvement of the adjacent RCL is not uncommon, and it is associated with a poor clinical outcome after nonsurgical treatment.[4,6] Understanding lateral elbow anatomy and footprints or bone attachments of the RCL and CET is therefore essential. The results of our study show that the mean RCL footprint measured 8.9 mm in length and comprised 54% of the combined humeral attachments of

Figure 2. Normal RCL in a cadaveric specimen. **A**, Sonogram over the lateral elbow in the coronal plane showing the RCL (deep to arrowheads) in the long axis from its humeral attachment, or footprint (between arrows), to the annular ligament (a; right side of image is distal). Note the CET (curved arrows), which is obliquely coursing superficial to the RCL. H indicates humerus; and R, radial head. **B**, Sonogram over the lateral elbow in the transverse plane showing the RCL (arrowheads) in the short axis within the intertubercular sulcus of the humerus and overlying the CET (curved arrow; left side of image is anterior). **C** and **D**, Corresponding sonograms after removal of the CET showing the RCL (arrowheads) and its humeral footprint (between arrows). Note the exposed CET footprint (open arrow). The RCL footprint measured 7.4 mm in length and comprised 48% of the combined RCL and CET footprints.

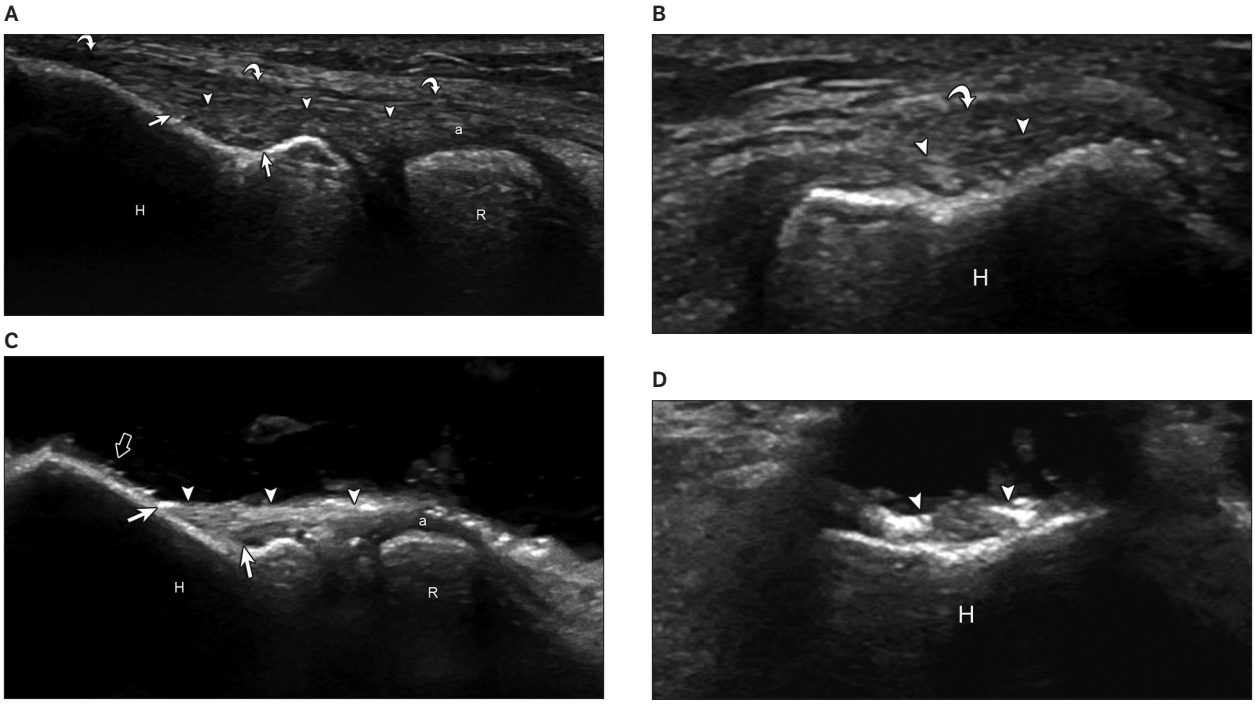

Figure 3. Normal RCL in a cadaveric specimen. **A**, Sonogram over the lateral elbow in the coronal plane showing the RCL (deep to arrowheads) in the long axis from its humeral attachment, or footprint (between arrows), to the annular ligament (a; right side of image is distal). Note the CET (curved arrows), which is obliquely coursing superficial to the RCL. H indicate humerus; and R, radial head. **B**, Corresponding sonogram after removal of the CET showing the RCL (arrowheads) and its humeral footprint (between arrows). Note the stump of the CET at its humeral footprint (open arrow). The RCL footprint measured 10 mm in length and comprised 62% of the combined RCL and CET footprints. **C**, Dissected lateral elbow specimen showing the RCL (arrows), annular ligament (a), and transected stump of the CET (black arrow; right side of image is distal).

A

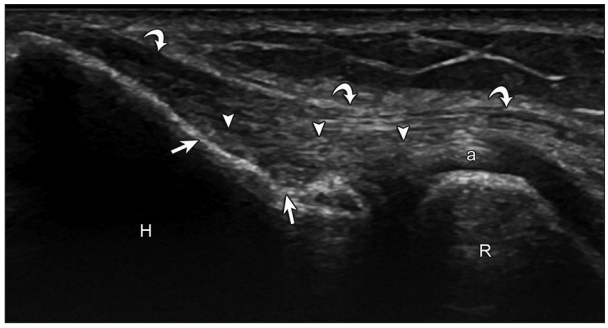

B

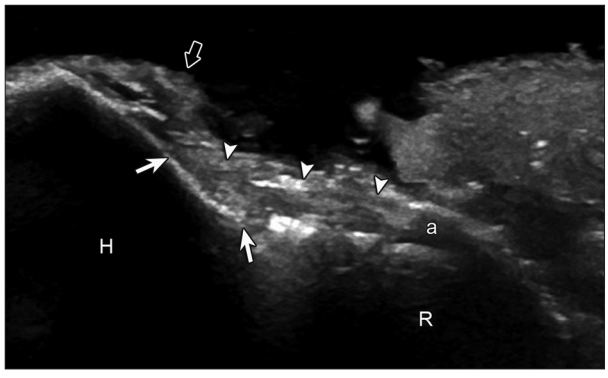

C

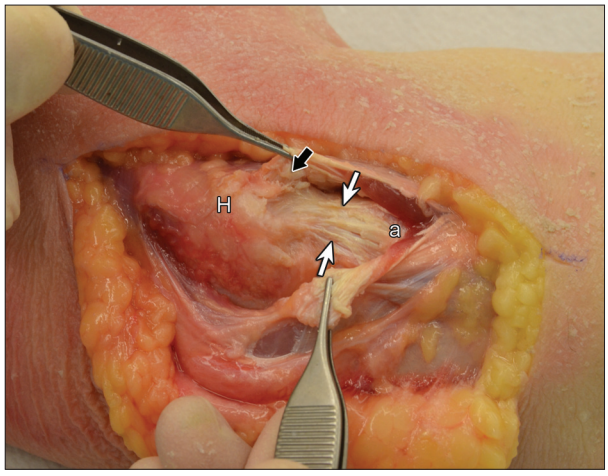

Figure 4. Normal RCL in 21-year-old male patient. **A** and **B**, Coronal T1-weighted MRI (**A**; TR/TE, 666/10 milliseconds; slice thickness, 2.5 mm) after the intra-articular administration of gadolinium showing the RCL (arrowhead) and its humeral attachment, or footprint, in the intertubercular sulcus (arrows). The overlying CET (curved arrow) courses obliquely relative to the CET from anterior to posterior, so that the next posterior image (**B**) shows the CET footprint (black arrows). H indicates humerus; R, radial head; and U, ulna. The RCL footprint measured 7.5 mm in length and comprised 43% of the combined RCL and CET footprints.

A

B

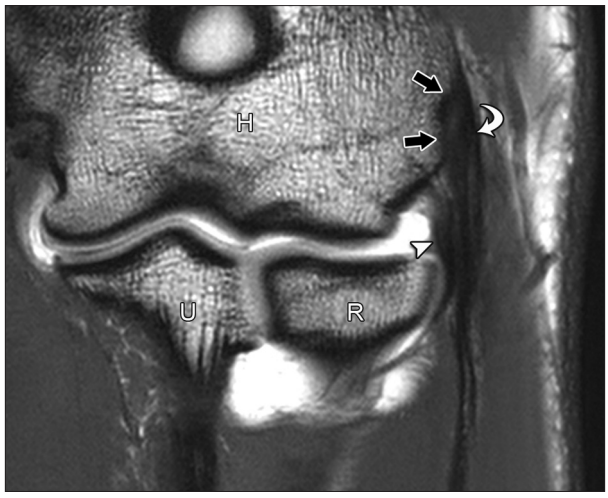

the CET and RCL. Knowledge of this anatomy allows an accurate assessment of an RCL abnormality in the setting of tennis elbow.

With regard to the anatomy of the lateral elbow, the CET is located superficial to the RCL and is comprised of the extensor carpi radialis brevis, the extensor digitorum communis, the extensor digiti minimi, and the humeral head of the extensor carpi ulnaris, with the extensor carpi radialis brevis located most anteriorly.[8] The RCL complex is comprised of the RCL proper, the annular ligament, and the lateral ulnar collateral ligament, with the latter extending from the radial collateral and annular ligaments to the crista supinator of the proximal ulna.[4,8] The RCL attaches to the humerus at the superior aspect of the intertubercular sulcus and the inferior aspect of the superior tubercle and extends distally to the annular ligament.[8] The footprints of the RCL and the CET lie adjacent to each other at the distal humerus, with the RCL footprint identified distal and deep to the CET footprint.[4,9] The long axis of the CET is slightly oblique to the long axis of the RCL; when moving from distal to proximal toward the humerus in the transverse plane, the CET crosses over the RCL and intertubercular sulcus from anterior to posterior to attach to the humerus.

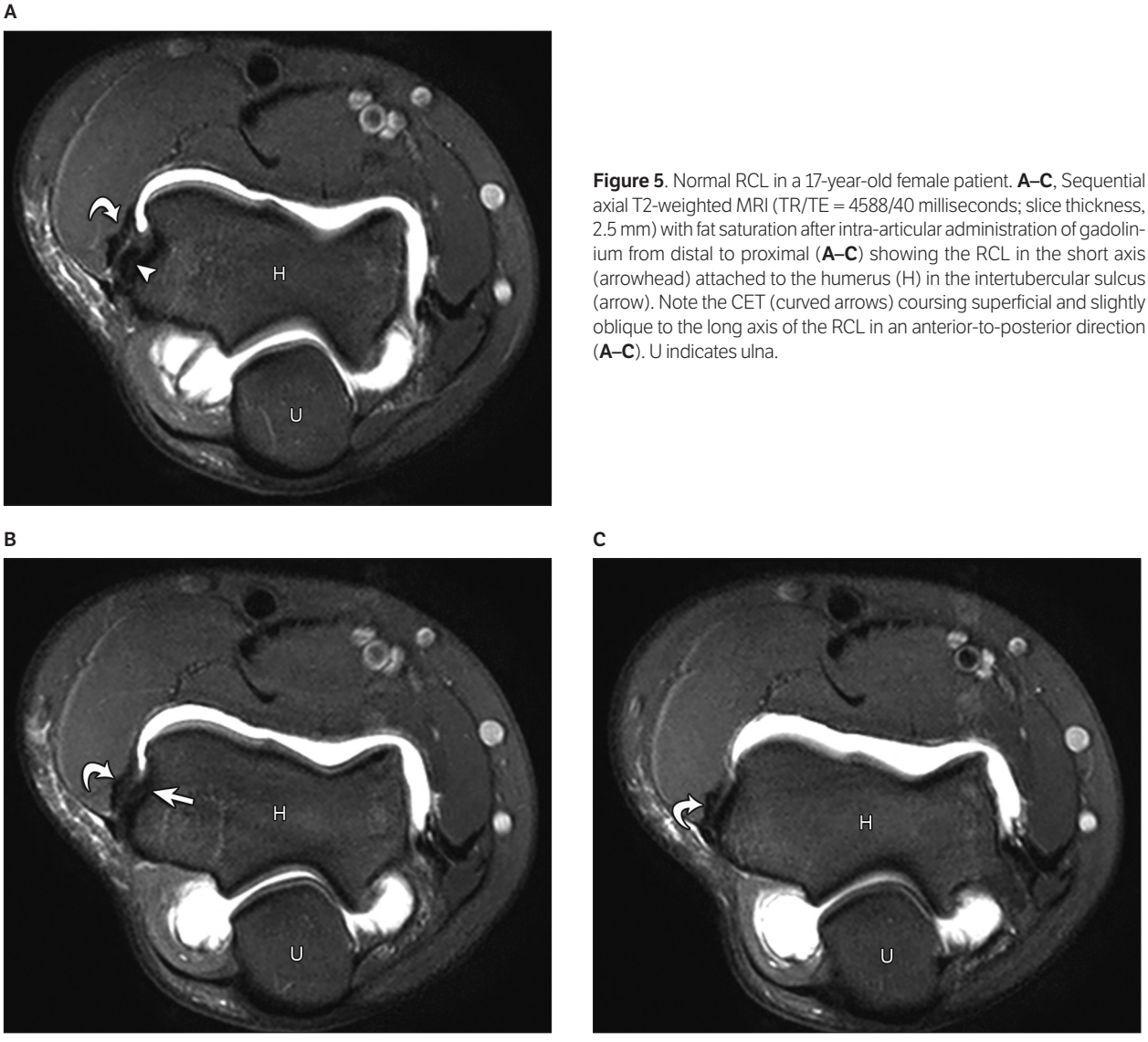

Figure 5. Normal RCL in a 17-year-old female patient. **A–C**, Sequential axial T2-weighted MRI (TR/TE = 4588/40 milliseconds; slice thickness, 2.5 mm) with fat saturation after intra-articular administration of gadolinium from distal to proximal (**A–C**) showing the RCL in the short axis (arrowhead) attached to the humerus (H) in the intertubercular sulcus (arrow). Note the CET (curved arrows) coursing superficial and slightly oblique to the long axis of the RCL in an anterior-to-posterior direction (**A–C**). U indicates ulna.

The pathologic findings of tennis elbow, or what is often clinically termed "lateral epicondylitis," include tendinosis and a possible tear of the CET at or near its humeral origin.[3] Histologic evaluation shows abnormalities of the CET, which include mucoid degeneration, neovascularization, fibroplasia, fibrocartilage formation, and possible dystrophic calcification.[3] Given the lack of acute or chronic inflammation, the term "tendinitis" is not accurate; therefore, the terms "tendinosis" and "tendinopathy" are used. On sonography, tendinosis appears as abnormal tendon hypoechogenicity with possible tendon thickening but without a well-defined defect.[10,11] Increased flow on color or power Doppler imaging is often present with tennis elbow, which represents neovascularity and not inflammation.[3] On MRI, tendinosis will appear as an abnormal increased gray or intermediate signal of the tendon with possible tendon thickening.[2] Interstitial tears may also be identified, which appear as anechoic clefts within the tendon on sonography and fluid signal clefts on MRI.[1] The presence of a large interstitial tear of the CET (8 mm in average size compared to 4 mm) has been shown to be associated with a poor response to nonsurgical management.[6]

Tennis elbow represents an overuse or sports-related injury in which there is degeneration (tendinosis or tendinopathy) and a possible tear of the CET.[2] Commonly presenting in patients in the fourth and fifth decades of life, the pain associated with tennis elbow may substantially interfere with activities of daily living and an individual's occupation.[2] Sonography and MRI are often used to confirm clinically suspected CET abnormalities and to exclude other causes of lateral elbow symptoms.[1] One possible etiology for such symptoms is posterior interosseous nerve syndrome, in which entrapment of the deep branch of the radial nerve at the supinator may occur.[1] Abnormalities of the RCL may also be found and are associated with a poor clinical outcome when combined with findings of lateral epicondylitis.[6]

The findings of our study characterize the location of the RCL footprint on the distal humerus, which allows distinction between the RCL and the CET as shown on sonography. The results of the cadaveric dissection and subsequent sonography showed that the mean RCL footprint length was 8.4 mm (range, 7.4–10.0 mm), or 54% of the combined RCL and CET footprints. These measurements are similar to measurements taken from the MR arthrograms, which showed a mean length of 9.1 mm (range, 6.4–12.5 mm), or 54% of the combined RCL and CET footprints. The slightly smaller measurements taken from the cadaveric specimens may have been related to a sampling error, given the low number of dissected specimens relative to the patients who underwent MR arthrography. A prior study reported that a linear echogenic interface between the CET and RCL can be seen on sonography, as well as a bone tubercle located between the CET and RCL humeral attachments.[4] These sonographic findings were not seen in our cadaveric specimens in the imaging plane where our measurements were obtained, although further studies with larger numbers of patients are needed to assess these findings.

When performing sonography of the lateral elbow, knowledge of the RCL and CET footprint measurements can assist in their identification as separate individual structures. Further distinction between the RCL and CET can be accomplished during real-time sonography, given knowledge of the anatomy and courses of these structures. Since the overlying CET courses slightly oblique to the long axis of the RCL, real-time scanning will often show the fibers of the CET and RCL moving in slightly different directions. These methods will allow accurate characterization of lateral elbow abnormalities in tennis elbow with regard to involvement of the RCL.

We acknowledge several limitations to this study, which included a limited number of cadaveric specimens and patients who underwent MR arthrography who also were in different age groups. In addition, we relied on imaging findings to identify patients with normal lateral elbows on arthrograms. Last, measurements were obtained by consensus without calculation of intraobserver and interobserver variability.

In conclusion, the RCL can be differentiated from the CET on sonography with knowledge of the RCL humeral footprint extent, which measured 8.9 mm in length and comprised 54% of the combined RCL and CET footprints.

References

1. Kotnis NA, Chiavaras MM, Harish S. Lateral epicondylitis and beyond: imaging of lateral elbow pain with clinical-radiologic correlation. *Skeletal Radiol* 2012; 1:369–386.
2. Walz DM, Newman JS, Konin GP, Ross G. Epicondylitis: pathogenesis, imaging, and treatment. *Radiographics* 2010; 30:167–184.
3. Potter HG, Hannafin JA, Morwessel RM, DiCarlo EF, O'Brien SJ, Altchek DW. Lateral epicondylitis: correlation of MR imaging, surgical, and histopathologic findings. *Radiology* 1995; 196:43–46.
4. Teixeira PA, Omoumi P, Trudell DJ, et al. Ultrasound assessment of the lateral collateral ligamentous complex of the elbow: imaging aspects in cadavers and normal volunteers. *Eur Radiol* 2011; 21:1492–1498.
5. Bredella MA, Tirman PF, Fritz RC, Feller JF, Wischer TK, Genant HK. MR imaging findings of lateral ulnar collateral ligament abnormalities in patients with lateral epicondylitis. *AJR Am J Roentgenol* 1999; 173:1379–1382.

6. Clarke AW, Ahmad M, Curtis M, Connell DA. Lateral elbow tendinopathy: correlation of ultrasound findings with pain and functional disability. *Am J Sports Med* 2010; 38:1209–1214.
7. Jacobson JA, van Holsbeeck MT. Musculoskeletal ultrasonography. *Orthop Clin North Am* 1998; 29:135–167.
8. Zoner CS, Buck FM, Cardoso FN, et al. Detailed MRI-anatomic study of the lateral epicondyle of the elbow and its tendinous and ligamentous attachments in cadavers. *AJR Am J Roentgenol* 2010; 195:629–636.
9. Capa-Grasa A, Rojo-Manaute JM, Rodriguez-Maruri G, de Las Heras Sanchez-Heredero J, Smith J, Martin JV. Selective 360° percutaneous extensor carpi radialis brevis tendon release for tennis elbow: an experimental study. *J Ultrasound Med* 2012; 31:1193–1201.
10. Levin D, Nazarian LN, Miller TT, et al. Lateral epicondylitis of the elbow: US findings. *Radiology* 2005; 237:230–234.
11. Connell D, Burke F, Coombes P, et al. Sonographic examination of lateral epicondylitis. *AJR Am J Roentgenol* 2001; 176:777–782.